Orientation Control of Graphene Flakes by Magnetic Field: Broad Device Applications of Macroscopically Aligned...

Article *in* Advanced Materials · November 2016

DOI: 10.1002/adma.201604453

14 authors, including:

Jonathan Hu
Baylor University

Keshab Dahal
University of Houston

Zhifeng Ren
Boston College, USA

Jiming Bao
University of Houston

ADVANCED MATERIALS
www.advmat.de

Orientation Control of Graphene Flakes by Magnetic Field: Broad Device Applications of Macroscopically Aligned Graphene

Feng Lin, Zhuan Zhu, Xufeng Zhou, Wenlan Qiu, Chao Niu, Jonathan Hu, Keshab Dahal, Yanan Wang, Zhenhuan Zhao, Zhifeng Ren, Dimitri Litvinov, Zhaoping Liu, Zhiming M. Wang, and Jiming Bao**

With rapid advances in 1D and 2D nanomaterials, it becomes important to develop techniques to control the orientation of individual nanostructures and eventually assemble them into functional macroscopic objects.[1–4] This is because the properties of low-dimensional materials are intrinsically anisotropic and adherent to their atomic structures.[5] Only when they are arranged in a macroscopic order, can unique properties of individual nanostructures be fully utilized and transformed into large-scale macroscopic functions.[1,3] Macroscopically ordered nanomaterials have many benefits in device applications, for example, by aligning billions of single-wall carbon nanotubes or nanowires in one direction, optical, electrical, and electronic properties of a single carbon nanotube (CNT) can be expanded to a whole wafer;[1,3,6] a collective response and alignment of graphene oxide flakes exhibits birefringence and has found applications in display and electro-optic switching;[7–11] when graphene flakes are assembled in the same planar direction, they show excellent thermal, optical, electrical, and electromagnetic shielding properties.[12–15] These macroscopic orientational orders of nanomaterials are typically achieved with three techniques: mechanical shear stress, electrical fields, or magnetic fields. Mechanical alignment is an old and general method that can be applied to almost every nanomaterial, but the control by a magnetic or electrical field offers more flexibility and is more suitable for device applications. Magnetic or electrical field alignment of most nanomaterials such as CNT, graphene oxide flakes, or 2D transition metal dichalcogenides has been achieved,[7,16] but similar alignment of graphene remains a challenge and has not been demonstrated, although theoretically study has been reported.[17,18]

Diamagnetism is a ubiquitous property of materials due to magnetic response of orbital electrons. Although high-quality graphite or highly ordered pyrolytic graphite (HOPG) has the highest diamagnetic susceptibility among bulk materials,[19] the diamagnetic property of graphene has not received much attention until recently.[18,20–22] Because of unique electronic band structure and high electron mobility, graphene exhibits higher susceptibility than graphite. Diamagnetism has been used to align nonmagnetic nanomaterials, but a huge field is typically required. For instance, a strong magnetic field of 45 T was used to align CNTs.[1,23,24] Smaller magnetic field has been used to align graphite and graphene flakes, but only with the assistance of magnetic or paramagnetic nanoparticles for enhanced electrical conductivity, thermal conductivity, and optical transparency.[13–15,25,26] These properties and associated device performances will be further improved if the magnetic alignment can be achieved with pure graphene or graphite flakes. In this work, we demonstrate for the first time the magnetic response and alignment of graphene flakes and, more importantly, that orientation control and alignment can be achieved with a weak

F. Lin, Dr. Y. Wang, Dr. Z. Zhao, Prof. Z. M. Wang, Prof. J. M. Bao
Institute of Fundamental and Frontier Sciences
University of Electronic Science and Technology of China
Chengdu, Sichuan 610054, China
E-mail: zhmwang@uestc.edu.cn; jbao@central.uh.edu

F. Lin, Z. Zhu, Dr. Y. Wang, Dr. Z. Zhao, Prof. D. Litvinov, Prof. J. M. Bao
Department of Electrical and Computer Engineering
University of Houston
Houston, TX 77204, USA

Prof. X. Zhou, Prof. Z. Liu
Ningbo Institute of Materials Technology and Engineering
Chinese Academy of Sciences
Ningbo, Zhejiang 315201, China

Prof. X. Zhou, Prof. Z. Liu
Key Laboratory of Graphene Technologies and Applications of Zhejiang Province
Ningbo Institute of Materials Technology and Engineering
Chinese Academy of Sciences
Ningbo, Zhejiang 315201, China

Dr. W. Qiu, Prof. D. Litvinov, Prof. J. M. Bao
Materials Science and Engineering
University of Houston
Houston, TX 77204, USA

C. Niu, Prof. J. Hu
Department of Electrical and Computer Engineering
Baylor University
Waco, TX 76798, USA

K. Dahal, Prof. Z. Ren
Department of Physics and TcSUH
University of Houston
Houston, TX 77204, USA

Prof. Z. M. Wang
State Key Laboratory of Electronic Thin Films and Integrated Devices
University of Electronic Science and Technology of China
Chengdu, Sichuan 610054, China

DOI: 10.1002/adma.201604453

magnetic field from small commercial magnets. As examples of novel device applications, we show that graphene flake suspension can be used for magnetic field sensing and magnetically controlled display.

Two types of graphene flakes were prepared. Few-layer (one to three layers, 2–6 µm in diameter) graphene flakes were obtained via electrochemical exfoliation of HOPG.[27] Multilayer graphene flakes with average thickness of 2.4 nm were synthesized via intercalation and exfoliation of graphite by Ningbo Morsh Technology Co., Ltd. Graphene flakes were dispersed in either de-ionized water in Figures 2, 3, 4, and 6 or in *N*-methyl-2-pyrrolidone (NMP) in Figures 1 and 5. Magnetic measurements were obtained using a Lakeshore 735 vibrating sample magnetometer. Graphene flakes were then dried and laminated for diamagnetic susceptibility measurement. **Figure 1**a shows the magnetization curves of two types of flakes when the magnetic field is perpendicular to the flake surfaces. Diamagnetic susceptibilities of 0.31×10^{-4} emu g^{-1} Oe^{-1} for few-layer graphene flakes and 0.23×10^{-4} emu g^{-1} Oe^{-1} for multilayer flakes are obtained. The susceptibility of few-layer graphene flakes is higher than that of original HOPG (0.05×10^{-4} emu g^{-1} Oe^{-1}) and reported single-layer graphene.[19–22] Such a high susceptibility indicates the high quality of graphene flakes and is desired for the magnetic alignment of their orientations.

When the surface of a diamagnetic graphene flake is oriented perpendicular to an external magnetic field, the induced magnetic field is in a direction opposite to the external field, leading to repulsive magnetic force and increased total interaction energy. In order to minimize the magnetic potential energy, the flake will rotate away from the field until its surface is in parallel with the external field. Graphene alignment using its diamagnetism was investigated theoretically, but a large field of 9 T was predicted,[18] and experimental demonstration has not been reported. To detect the magnetic response of few-layer graphene, we monitor the birefringence of its liquid suspension.[7,8,16,28] This is a typical technique to probe the orientations of liquid crystal molecules as well as layered 2D nanomaterials. Figure 1b shows the experimental setup where a horizontal magnetic field through graphene suspension in a cuvette is provided by permanent magnets. The magnetic response can be clearly seen from the change of the birefringence in the transmission images of Figure 1c–f. The alignment of graphene along the magnetic field is confirmed by the observations that the transmission is stronger in Figure 1d when both polarizers are 45° relative to the magnetic field but becomes weaker in Figure 1f where one polarizer is parallel and the other is perpendicular to the field. Figure 1c,e shows almost no difference when no magnetic field is applied.

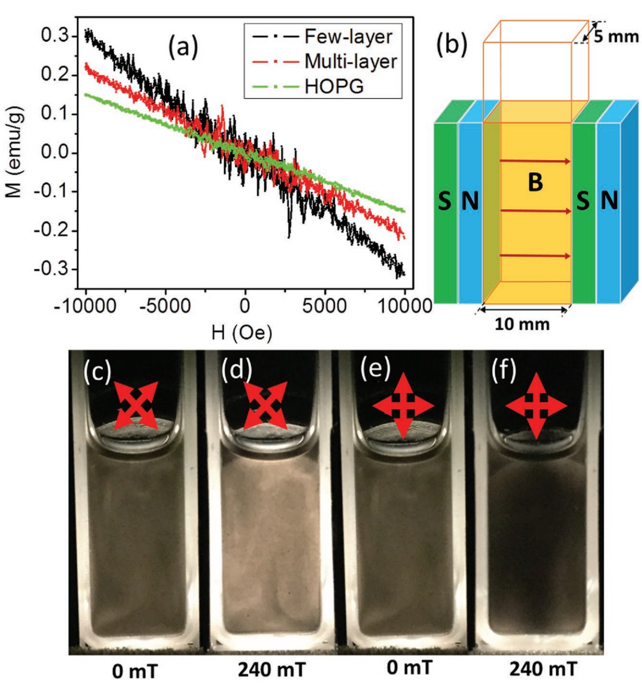

Figure 1. Diamagnetic susceptibility and magnetic field induced birefringence of graphene flakes. a) Diamagnetic susceptibilities of few-layer and multilayer graphene flakes as well as HOPG. b) Schematic of experimental setup. Horizontal magnetic field across the cuvette is provided by permanent magnets. Two polarizers are placed on the front and back sides of the cuvette. c–f) Birefringence images of few-layer graphene suspension between two crossed optical polarizers (red arrows indicate their polarizations) under zero and 240 mT magnetic field.

To observe the magnetic response of flakes in a more convenient way, we used suspension of multilayer graphene flakes in a plastic beaker and placed magnets directly below it. **Figure 2**a–c shows photographs of the suspension with 0, 1, and 2 bar magnets below, respectively. The magnetic response of graphene suspension can be immediately recognized by the bright–dark patterns created by magnets: The area right above the magnet surface remains dark, but the edge and surrounding regions of the magnets become bright. To determine the orientation of the flakes in these regions and understand the underlying mechanism, we took optical microscope images of selected areas of a diluted suspension. Figure 2e shows the photograph of graphene flakes in the center dark region in Figure 1b; narrow and dark images of flakes indicate that they are vertically oriented. Figure 2f shows that flakes are horizontally oriented, with some flakes even becoming parallel to the liquid surface and giving shiny specular reflections.

Based on these observations and the well-known magnetic field pattern of permanent magnets, we can conclude again that graphene flakes are aligned with the magnetic field, and orientations of flakes in three cases are illustrated in Figure 2g–i. Note that, around the middle of two magnets, the magnetic field and flakes are oriented horizontally. The reflection is relatively high in this case by horizontally oriented flakes. When the flakes are oriented vertically, the reflection is low as the light is transmitted and scattered among flakes. In the initial suspension, flakes are randomly oriented. The orientation-dependent dark to bright contrast is similar to the flakes of graphene oxides reported by the authors before,[8] which will be further explained in the text later. Note that magnetic alignment is completed when field passes through the surface of a flake, but the orientation of the flake is not totally fixed, and it can still rotate around the field direction. Because of this, some flakes in Figure 2f exhibit bright specular reflectance but many other flakes are not parallel to the surface, which still appear dark from the top view.

To better understand the dynamics of flakes under magnetic field, we monitor the orientation of a multilayer graphene flake in real time. **Figure 3** shows snapshots of its rotation dynamics; the video can be found in the Supporting Information. It can

Adv. Mater. **2016**,
DOI: 10.1002/adma.201604453

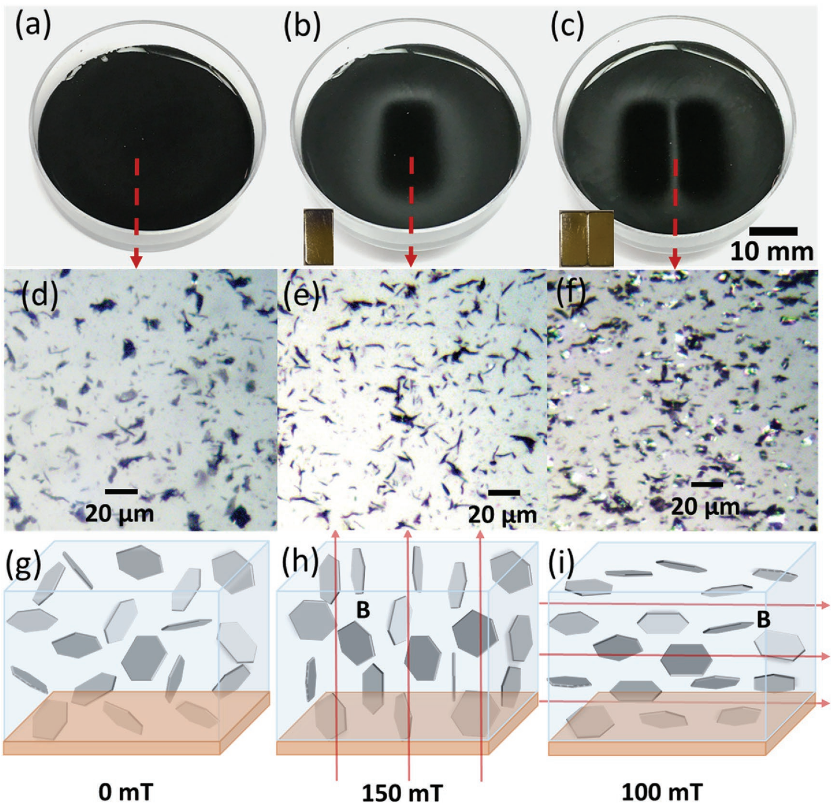

Figure 2. Magnetic field induced changes in optical reflectivity of a multilayer graphene suspension. a–c) Optical images of the suspension when zero, one, and two magnets placed underneath. Insets are optical images of the magnets. d–f) Optical microscope images and g–i) schematics of flake orientations of a diluted suspension from the region marked by red dashed lines in (a)–(c). The suspension in (d)–(f) is diluted in order to resolve individual flakes.

gravitational potential to turn and flip up, so a relatively strong field is required. After the removal of the field, the flake slowly returned to its original position in 10 s. A complete rotation video is available in the Supporting Information. With a high magnetic field of 100 mT, the rotation can be done within 0.5 s. This field is much weaker than the predicted 9 T, which is due to large size and mass of multilayer flakes.[18] For micro-sized few-layer graphene, we estimate a weak field of 10 mT in order to overcome thermal fluctuation energy at room temperature.

It is important to point out that although the magnetic alignment of diamagnetic flakes is similar to those of paramagnetic or ferromagnetic objects,[15] the above magnetic alignment of graphene flakes is due to their intrinsic diamagnetic susceptibility rather than magnetic impurities such as Fe, which is the most abundant element in graphite or graphene.[22] This conclusion is supported by the following discussions and new observations. First, the magnetic impurity level in our samples is too low to be detected by energy-dispersive X-ray spectroscopy (Figure S1, Supporting Information). Trace element analysis based on inductively coupled plasma (ICP) shows low Fe concentrations of 141.5 and 0.709 ppm for multilayer and few-layer graphene samples, respectively. This is expected because HOPG typically has a much lower impurity level than natural graphite.[22] More importantly, two magnetization curves in Figure 1 clearly show that the paramagnetic contribution is negligible for both graphene samples.[20,22] This clean and strong diamagnetic susceptibility can also be seen from magnetic levitation of disks made of graphene flakes in Figure S2 (Supporting Information). The last proof is that our graphene flakes are not attracted to magnets in all of our

be seen that the flake is initially laid flat at the bottom of the beaker. It was chosen for better imaging because a suspended flake is difficult to track and focus. After the application of a 24 mT vertical magnetic field, the flake began to turn and finally stood up vertically on one of its edges, in alignment with the magnetic field. Note that for this flake, it has to overcome the

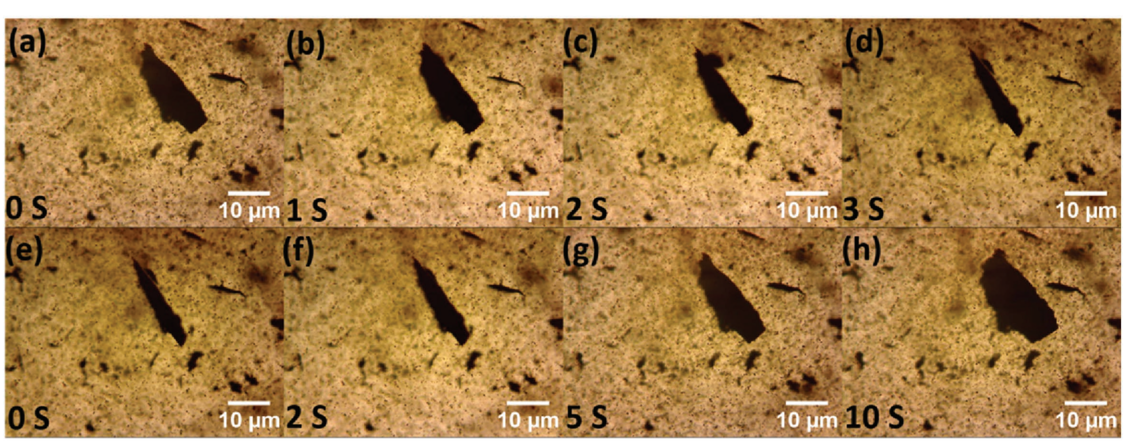

Figure 3. Dynamics of a multilayer graphene flake in water under a magnetic field. Top-down snapshots of a graphene flake after a–d) the application and e–h) removal of a vertical magnetic field. The video is available from the Supporting Information.

experiments, in contrast to those paramagnetic or ferromagnetic graphene flakes.[15]

Among numerous potential applications, we show two simple but totally novel applications based on bright–dark patterns created by magnets in Figure 2. Because of the sensitivity of graphene flakes to magnetic field, we can use them as magnetic field sensors. The field direction and strength can be read directly from optical images. The bright scattering part in suspension represents a horizontal magnetic field, while the black surface indicates a vertical magnetic field. Figure 2 is already a good example, but we want to determine the optimal concentration of graphene suspension that will produce the best bright to dark color contrast. **Figure 4**a–d shows the field pattern of the same magnet set with increasing graphene weight percentages from 0.01 to 0.2 wt%. For low concentration of 0.01 wt%, the suspension is semitransparent and the contrast is low. The contrast becomes much better with 0.1 wt%, and no obvious improvement with 0.2 wt%, so the concentration of 0.1 wt% is chosen for next field sensing display. Figure 4e shows a photograph of initial suspension without magnetic field, and Figure 4f–h shows the field patterns of different shapes and configurations of magnets. Polarizations of magnets are interleaved among nearby magnets. It can be seen that the field pattern resembles the configuration of magnets, but some subtle differences are also noticeable. For instance, in Figure 4f, the boundaries between four circular magnets become straight lines; in Figure 4g, only two center square patterns have the same size of actual magnets; all other patterns show expanded and distorted shape of magnets.

We claim that these patterns reflect the actual distribution of the magnetic field. Because of the small size of graphene flakes, graphene suspension is expected to provide higher spatial resolution than ordinary iron particles. This can be seen from the comparisons between patterns generated by graphene flakes and by iron particles in Figure S3 (Supporting Information). In fact, graphene suspensions have revealed subtle and fine features of the field that cannot be detected by iron particles. For example, the crossing of two bright lines at the center of four magnet corners is not a simple superposition; instead, all the centers appear dark, not bright. The lines actually do not cross each other; two new branches around the centers will form. This reflects the fact that magnets are not arranged in a perfectly symmetric square lattice and a magnetic field is a vector field without sources. In Figure 2h, the center bright line is not as straight as the physical boundary of two magnets, indicating internal nonuniformity of the magnetization. In addition, the patterns are formed immediately without any efforts, while the patterns by iron particle require careful spray and shaking of iron particles. More graphene field displays and simulations of field patterns can be found in Figures S4–S6 (Supporting Information).

Another straightforward application is a display without polarizing optics. This application is similar to what we have demonstrated with graphene oxide flakes,[8] but graphene has two important advantages. First, the display, in particular a reflective display, offers enough contrast with ambient light, so no additional lighting is needed.[8,29,30] Second, the display can be controlled by a magnetic field – a no-contact technique. The latter property allows us to package graphene suspension in a sealed window and then use a magnet to create arbitrary patterns. **Figure 5**a shows schematics of a graphene writing board and two methods that we use to write letters. Dark lines can be created by sliding a pole of a bar magnet on top of the writing board because it produces a magnetic field perpendicular to the board. A white line can be generated by the gap of two magnets because it produces horizontal magnetic field. Figure 5b,c shows the letters “IFFS” and “UESTC” written by these two methods. Note that the letters display the expected contrast, which is the same as in Figure 2. As demonstrated before, when transmission is imaged with back illumination, the dark letters appear bright, as shown in Figure 5d.

The orientation-dependent brightness of graphene flakes is a manifestation of its strong optical anisotropy.[8] To obtain a

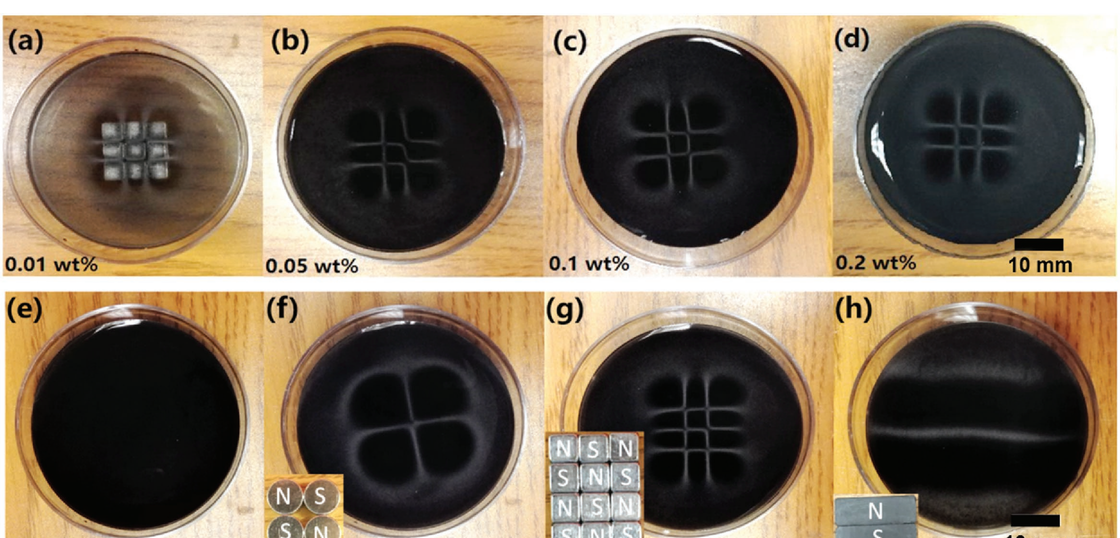

Figure 4. Multilayer graphene suspension for magnetic field sensing and display. a–d) Patterns generated by an array of nine cubic magnets using suspension with weight percentages of 0.01, 0.05, 0.1, and 0.2. e–h) Photographs of 0.1 wt% graphene suspension e) without magnetic field and f–h) with underneath magnets of different shapes and configurations shown in the insets.

Adv. Mater. 2016,
DOI: 10.1002/adma.201604453

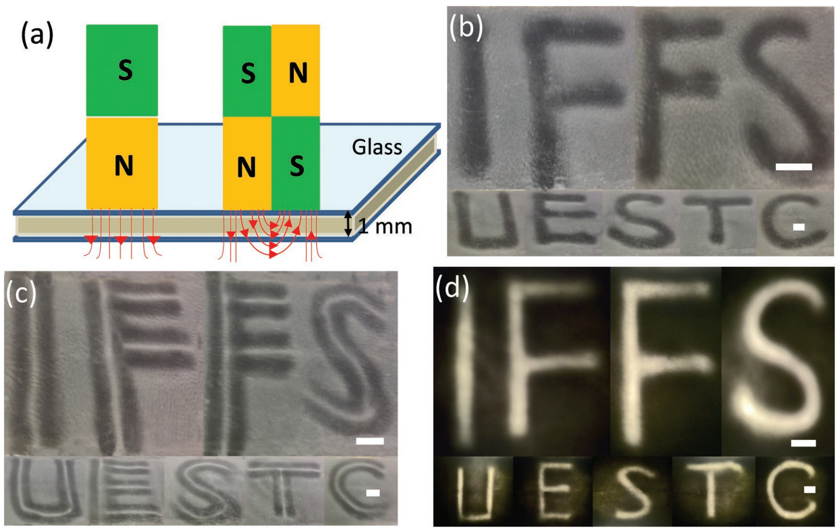

Figure 5. A graphene writing board with magnetic stylus. a) Operation principle. 0.1 wt% multilayer graphene suspension is filled between two glass windows. Each magnet produces 100 mT on its 5 × 5 mm^2 polar surface. b) Photographs of black letters written with a single magnet. c) Photographs of white–black letters written with double magnets. d) Photographs of back-illuminated letters written with a single magnet. Scale bars: 10 mm.

quantitative understanding, we took the spectra and compared them with simulations. **Figure 6**a shows the transmission spectrum of back-illuminated display cell with and without a vertical magnetic field. Figure 6b shows the reflection spectra of graphene flakes with a vertical, horizontal, and no magnetic field. The corresponding simulation results are shown in Figure 6c,d. It should be noted that we did not model the light source spectrum, and the experimental transmission and reflection spectra on vertical magnetic field are directly copied to Figure 6c,d. Hence, only the ratios of different curves in Figure 6c,d are explored in the simulation, which are the key to the experiment. Both the experiments and simulations reveal that transmission is strong but reflection becomes weak when flakes are vertically oriented. It is the opposite for flakes with surfaces perpendicular to the incident light. These observations and simulation results can be qualitatively understood from the relationship between the polarization of incident light and the graphene orientation. When the plane of a flake is perpendicular to the incident light, a large and uniform electron polarization is induced over the whole area of graphene, leading to the maximum absorption and reflection, hence minimum transmission. When a flake is vertically oriented as shown in the inset of Figure 6a, the flake will appear as a carbon nanotube or nanowire as in Figures 2e and 3d. Now there are two cases depending on the polarization of incident light with respect to the graphene plane. When the polarization is perpendicular to the graphene plane, the absorption and reflection is negligible because of weak induced electron polarization, similar to that for a carbon nanotube or nanowire.[6,31,32] When the polarization is aligned with the graphene plane, a slightly larger electron polarization is induced, but the absorption and reflection is still weak due to a much smaller physical cross section. Hence, in both cases when the flake is vertically oriented, the maximum transmission is achieved. The vertically and horizontally aligned flakes are two extreme cases, and randomly oriented flakes will have transmission and reflection in between. Details about simulation configuration and polarization dependent reflection/transmission can be found in Figure S7 (Supporting Information).

In summary, we have shown a high diamagnetism of exfoliated graphene and demonstrated its orientational response to magnetic field. We also showed huge anisotropic optical transmission and reflectivity of graphene flakes with simulations and experiments. By combining macroscopic alignment with anisotropic optical property of graphene, we demonstrated two novel device applications of graphene in magnetic field sensing

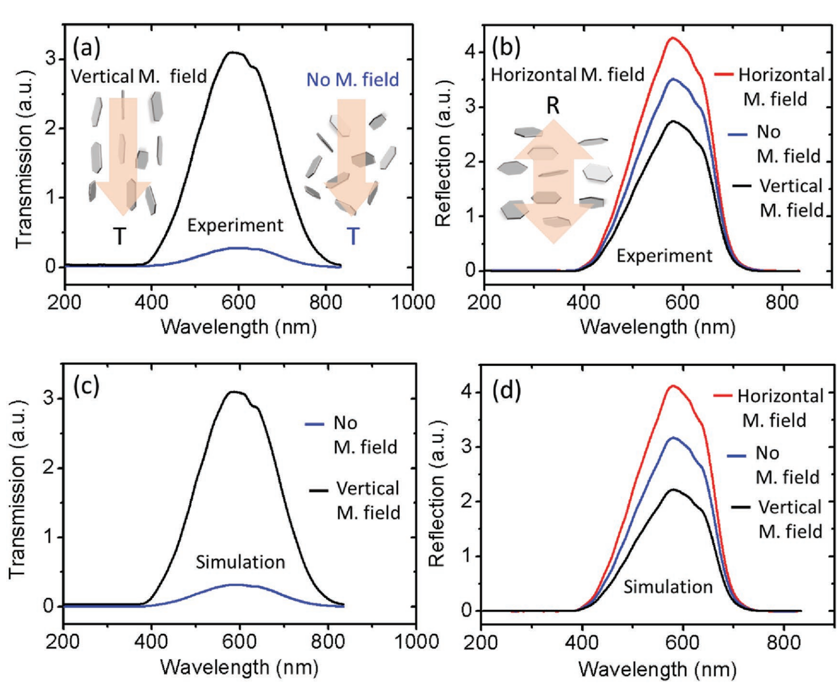

Figure 6. Orientation-dependent relative optical transmission and reflection of graphene flakes. Spectra are not normalized to the incident white light. M: magnetic. a) Transmission spectra of graphene flakes (black curve) with and (blue curve) without a vertical magnetic field. Insets: Schematics of orientations of flakes. T: transmission. b) Reflection spectra of graphene flakes with (red curve) horizontal magnetic field, (black curve) vertical magnetic field, and (blue curve) no field. Inset: Schematic of flake orientation under the horizontal magnetic field. R: reflection. c,d) Simulated spectra for experiments in (a) and (b).

and magnetic field controlled display. These devices can be readily used for educational demonstration and can be further improved for commercial applications. Magnetic alignment is safer and less invasive than electrical alignment, especially for nonmagnetic materials in conductive solvents. By mixing graphene with other nanomaterials, it is possible to align composites with a magnetic field. A complete alignment of graphene flakes can also be achieved using a rotating magnetic field.[2] The electrical control of orientation can be realized using micro-electromagnets.[33] Because graphene has shown enormous potential applications due to its versatile and superior properties, our demonstration not only provides us with a tool to control these properties with external field but also enables us to assemble graphene into macroscopic objects that preserve the excellent microscopic properties of graphene. Thus, our work has opened wider new applications of graphene and other nanomaterials.

Experimental Section

Sample Preparation: HOPG (EYGS121803) with thickness of 25 µm was purchased from Panasonic Electronic Device Co., Ltd. Few-layer graphene flakes were fabricated by electrochemical exfoliation of HOPG and multilayer graphene flakes were provided by Ningbo Morsh Technology Co., Ltd with intercalation and exfoliation of natural graphite flakes. The graphene writing board cell consisting of two glasses was sealed with 1 mm Polydimethylsioxane (PDMS) and filled with 0.1 wt% graphene NMP dispersion.

Magnetic Measurement: The magnetic curves of graphene were measured by using Lakeshore 735 vibrating sample magnetometer with dried graphene laminates mounted to the probe. The Fe impurity concentration in multilayer graphene flakes was measured with a Perkin-Elmer Optima 2100 Inductively Coupled Plasma-Atomic Emission Spectrometry (ICP-AEM); a Varian 810 ICP-MS (mass spectroscopy) was used to analyze few-layer graphene samples.

Supporting Information

Supporting Information is available from the Wiley Online Library or from the author.

Acknowledgements

F.L. was supported by Academic Exchange Special Fund from University of Electronic Science and Technology of China. J.M.B. acknowledges support from the National Science Foundation (CAREER Award ECCS-1240510) and the Robert A. Welch Foundation (E-1728). F.L. and J.M.B. thank Lixuan Shi of Beijing Normal University, Youyang Luo of Nankai University, and Rui Guo of Florida International University for assistance with the experiment. J.H. acknowledges support from the Vice Provost for Research at Baylor University.

Received: August 21, 2016
Revised: September 19, 2016
Published online:

[1] D. A. Walters, M. J. Casavant, X. C. Qin, C. B. Huffman, P. J. Boul, L. M. Ericson, E. H. Haroz, M. J. O'Connell, K. Smith, D. T. Colbert, R. E. Smalley, *Chem. Phys. Lett.* **2001**, *338*, 14.
[2] R. M. Erb, R. Libanori, N. Rothfuchs, A. R. Studart, *Science* **2012**, *335*, 199.
[3] G. H. Yu, A. Y. Cao, C. M. Lieber, *Nat. Nanotechnol.* **2007**, *2*, 372.
[4] A. Akbari, P. Sheath, S. T. Martin, D. B. Shinde, M. Shaibani, P. C. Banerjee, R. Tkacz, D. Bhattacharyya, M. Majumder, *Nat. Commun.* **2016**, *7*, 12.
[5] F. Bonaccorso, Z. Sun, T. Hasan, A. C. Ferrari, *Nat. Photonics* **2010**, *4*, 611.
[6] X. W. He, W. L. Gao, L. J. Xie, B. Li, Q. Zhang, S. D. Lei, J. M. Robinson, E. H. Haroz, S. K. Doorn, W. P. Wang, R. Vajtai, P. M. Ajayan, W. W. Adams, R. H. Hauge, J. Kono, *Nat. Nanotechnol.* **2016**, *11*, 633.
[7] T. Z. Shen, S. H. Hong, J. K. Song, *Nat. Mater.* **2014**, *13*, 394.
[8] L. Q. He, J. Ye, M. Shuai, Z. Zhu, X. F. Zhou, Y. A. Wang, Y. Li, Z. H. Su, H. Y. Zhang, Y. Chen, Z. P. Liu, Z. D. Cheng, J. M. Bao, *Nanoscale* **2015**, *7*, 1616.
[9] Z. Xu, C. Gao, *Acc. Chem. Res.* **2014**, *47*, 1267.
[10] B. Dan, N. Behabtu, A. Martinez, J. S. Evans, D. V. Kosynkin, J. M. Tour, M. Pasquali, I. I. Smalyukh, *Soft Matter* **2011**, *7*, 11154.
[11] F. Lin, X. Tong, Y. A. Wang, J. M. Bao, Z. M. M. Wang, *Nanoscale Res. Lett.* **2015**, *10*, 16.
[12] W. L. Song, M. S. Cao, M. M. Lu, J. Yang, H. F. Ju, Z. L. Hou, J. Liu, J. Yuan, L. Z. Fan, *Nanotechnology* **2013**, *24*, 10.
[13] H. Babaei, P. Keblinski, J. M. Khodadadi, *Int. J. Heat Mass Transfer* **2013**, *58*, 209.
[14] H. Le Ferrand, S. Bolisetty, A. F. Demirörs, R. Libanori, A. R. Studart, R. Mezzenga, *Nat. Commun.* **2016**, *7*, 12078.
[15] B. Genorio, Z. W. Peng, W. Lu, B. K. P. Hoelscher, B. Novosel, J. M. Tour, *ACS Nano* **2012**, *6*, 10396.
[16] D. Rossi, J. H. Han, W. Jung, J. Cheon, D. H. Son, *ACS Nano* **2015**, *9*, 8037.
[17] Z. Wang, *Carbon* **2009**, *47*, 3050.
[18] Y. Ominato, M. Koshino, *Phys. Rev. B* **2013**, *87*, 8.
[19] D. Fischbach, *Phys. Rev.* **1961**, *123*, 1613.
[20] Z. L. Li, L. L. Chen, S. Meng, L. W. Guo, J. Huang, Y. Liu, W. J. Wang, X. L. Chen, *Phys. Rev. B* **2015**, *91*, 5.
[21] L. L. Chen, L. W. Guo, Z. L. Li, H. Zhang, J. J. Lin, J. Huang, S. F. Jin, X. L. Chen, *Sci. Rep.* **2013**, *3*, 2599.
[22] M. Sepioni, R. R. Nair, S. Rablen, J. Narayanan, F. Tuna, R. Winpenny, A. K. Geim, I. V. Grigorieva, *Phys. Rev. Lett.* **2010**, *105*, 207205.
[23] S. Zaric, G. N. Ostojic, J. Kono, J. Shaver, V. C. Moore, M. S. Strano, R. H. Hauge, R. E. Smalley, X. Wei, *Science* **2004**, *304*, 1129.
[24] L. R. Bornhoeft, A. C. Castillo, P. R. Smalley, C. Kittrell, D. K. James, B. E. Brinson, T. R. Rybolt, B. R. Johnson, T. K. Cherukuri, P. Cherukuri, *ACS Nano* **2016**, *10*, 4873.
[25] C. Zhou, W. Huang, Z. Chen, G. Ji, M. L. Wang, A. Chen, H. W. Wang, *Compos. Part B: Eng.* **2015**, *70*, 256.
[26] J. Billaud, F. Bouville, T. Magrini, C. Villevieille, A. R. Studart, *Nat. Energy* **2016**, *1*, 16097.
[27] K. Parvez, Z. S. Wu, R. J. Li, X. J. Liu, R. Graf, X. L. Feng, K. Müllen, *J. Am. Chem. Soc.* **2014**, *136*, 6083.
[28] N. Behabtu, J. R. Lomeda, M. J. Green, A. L. Higginbotham, A. Sinitskii, D. V. Kosynkin, D. Tsentalovich, A. N. G. Parra-Vasquez, J. Schmidt, E. Kesselman, Y. Cohen, Y. Talmon, J. M. Tour, M. Pasquali, *Nat. Nanotechnol.* **2010**, *5*, 406.
[29] D. K. Yang, J. W. Doane, Z. Yaniv, J. Glasser, *Appl. Phys. Lett.* **1994**, *64*, 1905.
[30] B. Comiskey, J. D. Albert, H. Yoshizawa, J. Jacobson, *Nature* **1998**, *394*, 253.
[31] H. E. Ruda, A. Shik, *Phys. Rev. B* **2005**, *72*, 115308.
[32] J. F. Wang, M. S. Gudiksen, X. F. Duan, Y. Cui, C. M. Lieber, *Science* **2001**, *293*, 1455.
[33] C. S. Lee, H. Lee, R. M. Westervelt, *Appl. Phys. Lett.* **2001**, *79*, 3308.